ESCUELA DE CONSTRUCCIÓN CIVIL
FACULTAD DE INGENIERÍA
Revista de la Construcción
Journal of Construction

Research Article

Performance of composite shear walls strengthened with FRP and subjected to blast load

Mahdi Hosseini[1,2,*], **Haitao Li**[1,2,*], **Ahmad Hosseini**[3], **Pritam Ghosh**[3]

1 College of Civil Engineering, Nanjing Forestry University, Nanjing (China); civil.mahdi.hosseini@gmail.com, lhaitao1982@126.com
2 Joint International Research Laboratory for Bio‑composite Building Materials and Structures, Nanjing Forestry University, Nanjing (China), lhaitao1982@126.com
3 Fiber Composite Laboratory, Hindustan Institute of Technology and Science, Chennai (India); ahmad.hosseini.ace@gmail.com, pritamrajghosh@gmail.com
*Correspondence: civil.mahdi.hosseini@gmail.com, lhaitao1982@126.com

Received: 28.07.2022; **Accepted:** 09.06.2023; **Published:** 31.08.2023

Citation: Hosseini, M., Li, H., Hosseini, A. and Ghosh, P. (2023). Performance of Composite Shear Walls Strengthened with FRP and Subjected to Blast Load. Revista de la Construcción. Journal of Construction, 22(2), 431-454. https://doi.org/10.7764/RDLC.22.2.431.

Abstract: The present paper aims to explore the performance of composite shear walls reinforced with Fiber Reinforced Polymer (FRP) sheets, subjected to blast loads. The finite-element method (FEM) implemented in the ABAQUS software is used to evaluate several numerical models to meet this objective. The parametric behavior of the system under the effect of blast load intensity was investigated, along with the FRP sheet material, concrete compressive strength, and also the geometric characteristics of wall components such as its thickness, spacing of FRP sheets, and thickness of the cross-sectional shape of the steel plates under the effect of blast load. It was found that the reinforcement of the composite shear wall by incorporating FRP sheets not only increases the stress absorption in the wall but also increases the load transfer capacity and leads to high energy dissipation using the polymer fibers. It has been found that carbon polymer sheets (CFRP) and glass polymer sheets (GFRP) have, respectively, the best and the weakest performance in shear wall stress absorption compared to AFRP sheets, and this is due to the tensile strength and low density of CFRP sheets. As the thickness of FRP sheets increases, the stress, strain and displacement created in the composite shear wall decrease, owing to the increase of the final strength, which is, in turn, the result of the increase in fiber thickness.

Keywords: Blast load, composite shear wall, finite element analysis, FRP sheet.

1. Introduction

Shear walls are among the most common structural elements to strengthen structures against lateral forces. There are two primary types of structural systems: reinforced concrete walls and steel shear walls. For example, the Yiwu Tower, situated in Yiwu, China, is a 156-meter-tall building comprising 38 floors. The architectural visualization and construction of this tower involved the utilization of a rectangular multi-partition structure made from a composite shear wall filled with concrete. While these systems are commonly used in conventional structures, they are not considered ideal for tall buildings that must withstand significant lateral forces. The utilization of reinforced concrete shear walls in such cases leads to thickening of the walls, resulting in reduced usable space and increased overall weight of the structure (Thorburn et al., 1983, Timothy and McCormick, 2010, Chen et al., 2015). On the other hand, using steel shear walls to handle lateral forces in tall structures is

not recommended due to weaknesses in areas under compressive stress and buckling. These weaknesses result in a reduced load-bearing capacity and compromised energy absorption of the wall (Wagner, 1935, Zhao et al., 2016). However, an effective solution to this problem is the simultaneous use of concrete and steel plates as composite shear walls. This type of wall combines the advantages of concrete and steel materials (Zhang et al., 2016). It possesses high shear strength and excellent ductility, enabling it to withstand high compressive and reciprocating lateral forces. As a result, it is deemed a suitable lateral load-bearing system for tall structures (Kulak et al., 1998, Ji et al., 2013).

Composite shear walls are divided into two types: (a) the composite shear walls cover the steel plate in the core and two concrete layers, and (b) the concrete core is covered with two layers of steel plates (Zhao & Astaneh-Asl, 2004, Nie et al., 2014). Using the existing standard codebooks, nowadays, designers design tall structures equipped with composite shear walls that can resist earthquake force (Moghimi & Driver, 2015). However, still, there is a lack of sufficient knowledge about the behaviour of shear walls against severe impact loads, such as blast loads (Warn & Bruneau, 2009).

A blast is typically characterized as a sudden and substantial release of energy. Similarly, blast loads are classified as severe lateral impact loads that differ from the dynamic bearing loads experienced by a structure (Nie et al., 2013, Hosseini et al., 2023). These loads are applied over a short duration and can result in significant structural damage, up to complete destruction and rupture of the structural support. (Khizab et al., 2021) utilized ABAQUS software to design moment-resisting frame structures of different heights with and without steel plate shear walls. They then extracted a two-dimensional side frame to analyze the impact of explosive loading. The findings revealed that the dual system of steel plate shear walls demonstrated favorable performance compared to the moment-resisting frame in the specific scenario of "blast in-plane frame". While examining the response of the shear wall designed for seismic loads to the load caused by the blast, Warn et al. (2009) have proposed an approximate method for estimating the Off-plate resistance in the wall sheet. Since it is practically impossible to design different members of structures in the face of large blasts, it is, therefore, essential to provide conditions to prevent the total rupture of the structures subject to blast in new designs (Jayasooriya et al., 2009, Shabanlou et al., 2021).

One of the standard methods for designing blast-proof composite shear walls is using reinforcement sheets such as FRP sheets to reinforce various components of structures (Hosseini et al., 2022, Mohamed et al., 2022, Liang et al., 2021, Wilt et al., 2023). Mutalib et al. (2011) used numerical analysis to investigate the behavior of concrete panel joints (RC) reinforced with FRP composites against blast load. They concluded that anchoring the FRP sheet prevented damage to the concrete wall covering and increased the capacity of FRP-reinforced RC walls against the blast loads.

Dan. (2012) employed experimental studies to investigate the performance of shear walls reinforced with CFRP fibers and concluded that using CFRP sheets increases the bearing wall by 20%, compared to the sample without such reinforcement. Improvements with FRP sheets have been used for decades to increase the resistance of various components of structures to static and quasi-static loads and dynamic loads such as earthquake and blast loads.

Although the use of these materials to strengthen beams and columns has become widespread in the past few years, it is agreed that the existing knowledge and experience related to using such materials in supporting composite shear walls is limited. Therefore, the study of the behaviour of composite shear walls against blast loads and their reinforcement using FRP fibres has become one of the topics of interest to researchers in recent years, leading to extensive numerical and laboratory studies in this field. (Rafiei et al., 2013) verified a finite element (FE) models designed to replicate the performance of a unique composite shear wall system. The system is composed of two profiled steel sheets as outer layers and a concrete core, designed to withstand in-plane loads. The purpose of this novel walling system is to serve as shear elements capable of effectively countering lateral loads in steel-framed buildings. (Epackachi et al., 2014) conducted experimental and numerical analysis on four flexure-critical SC (steel-concrete) walls under cyclic in-plane loading. These walls have an aspect ratio of 1.0. The study investigates various design parameters such as the thickness of the infill concrete, reinforcement ratio, spacing of studs, and spacing of tie bars. To facilitate the analysis, numerical models of these walls are created using the LS-DYNA FE tool.

(Askarizadeh & Mohammadizadeh, 2017) focused on enhancing the strength of reinforced concrete shear walls using FRP and steel strips. Numerical simulations and experimental investigations are conducted on half-scale walls subjected to cyclic loading. Both the numerical and experimental outcomes demonstrate that the incorporation of CFRP and steel strips enhances the structural resistance, capacity, and ductility.

Previous research studies have demonstrated the efficacy of composite shear walls and FRP sheets in fortifying structures against blast loads. However, limited attention has been given to the design and numerical analysis of the response of composite shear walls reinforced with FRP sheets under blast loads. It is imperative to identify the system and components of different structures, particularly composite shear walls, and evaluate their responses when subjected to blast loads. Such investigations are essential for achieving an optimal design of this system. The main purpose of this study is to investigate the behaviour of composite shear walls as a resistant lateral load system and its reinforcement with FRP sheets for resisting blast loads.

For this purpose, the behaviour of this type of wall was evaluated by performing numerical modelling of composite shear walls with FRP sheets, based on the nonlinear FE method and explicit dynamic analysis in ABAQUS and through conducting parametric studies. In this context, a comprehensive investigation has examined the impact of different design parameters on the performance of composite shear walls reinforced with FRP sheets under blast loading. These design parameters include blast load intensity, the material composition of the FRP sheets, compressive strength of concrete, and geometric characteristics of wall components such as the thickness and spacing of FRP sheets, along with the thickness and cross-sectional shape of steel plates.

2. Methodology

The present study was conducted by performing numerical modelling of composite shear walls with FRP sheets, using the finite element (FE) method in ABAQUS under the effect of blast loads. Moreover, dynamic load analysis with a fast increment rate or explicit dynamic analysis using the finite element method was employed to simulate blast loading.

2.1. *Dynamic explicit analysis*

Dynamic explicit analysis helps solve a wide range of nonlinear structural mechanics problems. This type of analysis is very accurate for modelling at short intervals to record the high-frequency characteristics of shock and blast wave load and determine the structure response. The explicit method allows us to evaluate the nonlinear effects of materials and the geometry of the problem (Ajimituhuo et al., 2018). The explicit method is beneficial and practical for modelling dynamic problems in time and frequency, such as impact analysis and seismic effects. It is also used extensively for nonlinear problems, including changing contact conditions.

2.2. *Modeling and validation*

In the present paper, the composite shear wall model used in the experimental study of X. Ji et al. (2013) has been adapted to develop the required model for analysis. This model includes a with-holes steel plate with a length of 1100 mm, a height of 2600 mm and a thickness of 3 mm, connected by bolts with a diameter of 8 mm and a length of 150 mm. The columns surrounding the steel plates consisted of a rectangular box column measuring 220 x 140 mm with a thickness of 4 mm and a height of 2600 mm. Additionally, a tubular steel column with a diameter of 89 mm, a thickness of 3.5 mm, and a height of 2600 mm was positioned inside it. The composite shear wall is placed on a foundation with dimensions of 750 x 600 mm and a length of 2800 meters, and a concrete beam with dimensions of 300 x 300 mm with a length of 1200 mm was formed on top of it. The geometry and details of the experimental model in the present paper are derived from the experimental model and are shown in Fig. 1.

After developing the initial model, the behaviour of the composite shear wall sample under the effect of cyclic lateral loading and axial compressive loading has been verified using numerical modelling. To meet this objective, ABAQUS / CAE Standard graphic software was employed. Solid elements were used to model the members of the perimeter frame, as well as the steel shear wall plate, to determine the modelling geometry. The type of elements, including Line (1-D), Shell (2-D) or Solid (3-D) were considered. The model comprises several parts; thus, the whole model was defined by defining the interaction between different parts, using connecting elements. In the laboratory model of Ji et al. (2013), eight parts, including steel box columns, steel pipe columns, with-holes steel plates, concrete walls, bolts, concrete foundations, concrete beams and both conventional and U-shaped reinforcements, were used to build the model. Notably, these sections were also simulated in the numerical model. The simulation of the geometry of the under-study model and the interaction between different model members are shown numerically in Fig.2 a and b, respectively.

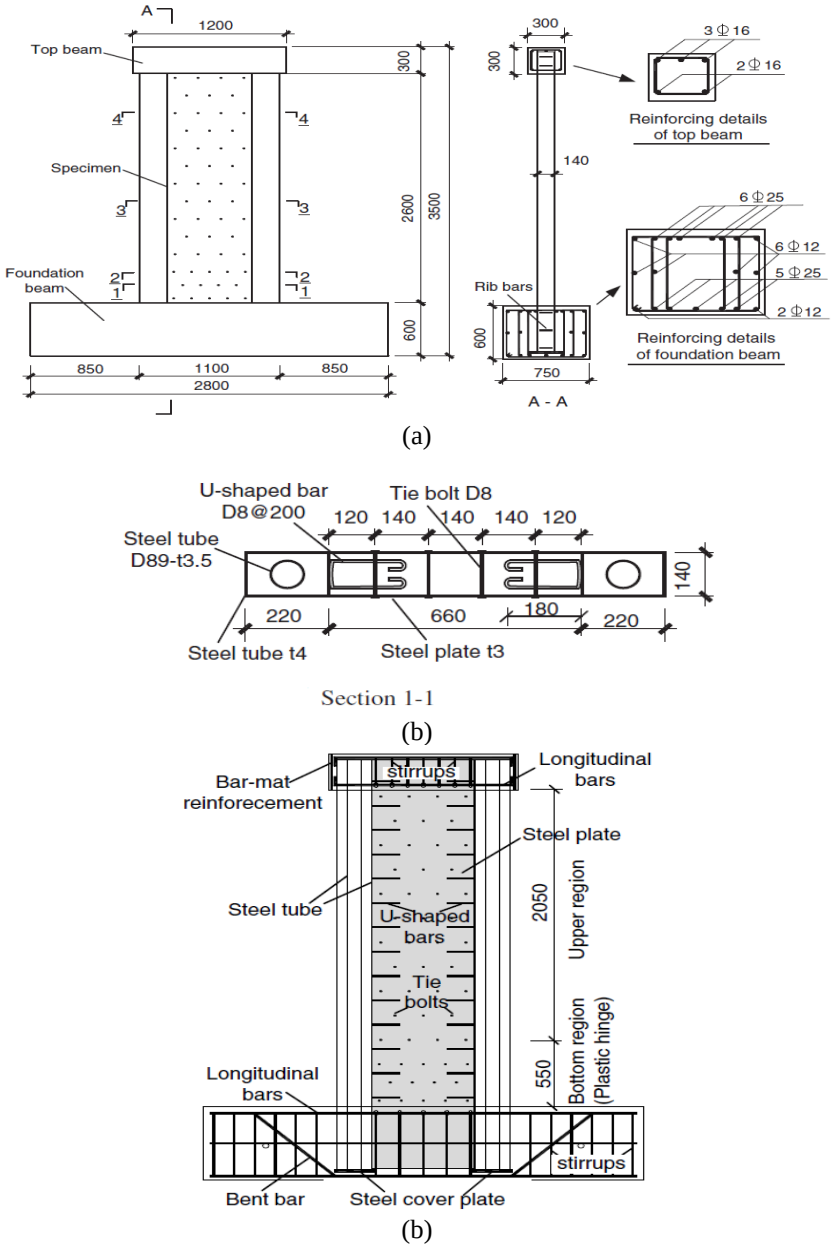

Figure 1. Composite shear wall for validation taken from experimental model, (a) model geometry, (b) model details (Ji et al., 2013).

2.3. *Boundary conditions, meshing and component integration*

In the experimental model, a fixed support condition was assumed. To create trapped conditions in the numerical model, all degrees of freedom except rotation around the desired axes were restricted, and also, the resistance outside the plane was modelled by closing the displacement in that direction (Fig. 2c). A cube node element was also used to mesh the model (Fig. 2d).

The C3D8R element considers large rotations and FE strains more accurately, making it possible to easily change the numerical model's thickness. Therefore, it is suitable for analyzing models with large strains, materials whose effective Poisson ratio is non-zero, and in cases where geometric nonlinearity of materials may occur (Shirinzadeh & Haghollahi, 2016). The cross-sectional characteristics are calculated using multiple four-node integrals in the plate thickness. The C3D8R element uses a reduced integration method, only using one integration point in the center of the page. This method can produce

more accurate results while significantly reducing the analysis time compared to the case of using elements in which the integration is performed entirely, especially in three-dimensional problems.

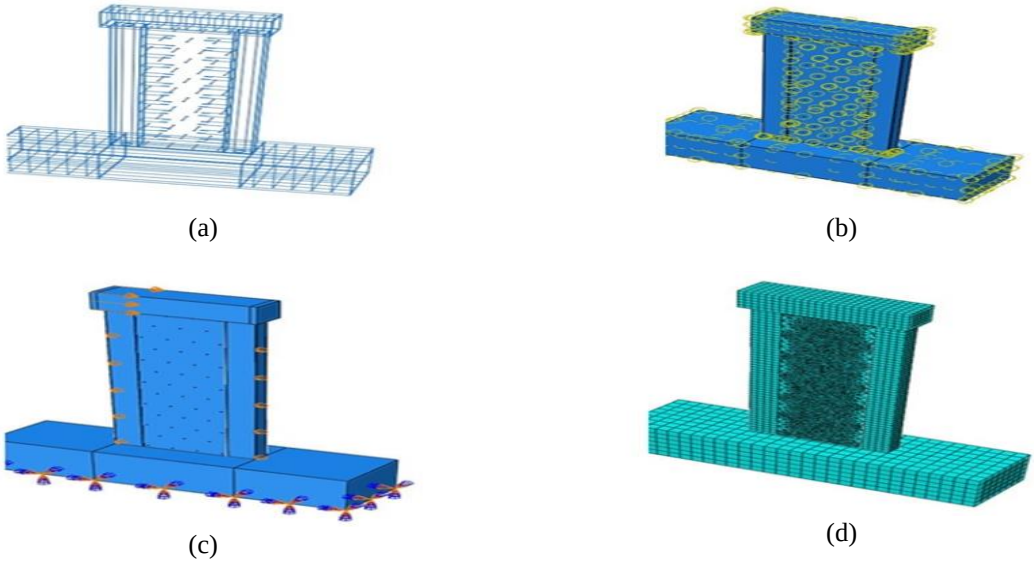

Figure 2. a) Numerical model geometry, b) interaction between different members of the model, c) boundary conditions, d) mesh model construction.

2.4. Boundary conditions, meshing and component integration

To show complete cyclic behavior, the three types of steel used in the experimental sample were also included in the numerical simulation, and the Von Mises stress contour was employed to analyze their behavior. Since only the uniform standard test is used, the definition of nonlinear material properties for the analytical sample requires some hypotheses. In ABAQUS, the plastic properties of materials can be incorporated either by isotropic hardening (in which the flow surface expands when plastic strains are tolerated) or by kinematic hardening (in which the flow surface is transferred without spreading during plastic strains). In the present paper, the isotropic hardening method is used to express the stress-strain behavior of the sheet and the frame members.

Table 1 displays the mechanical properties of the shear wall, considering the presence of various steel components such as beams, columns, wall panels, and bolts. It is important to note that each element possesses slightly different material properties. Fig. 3 contains an overview of the stress-strain diagram of concrete. According to this figure, the concrete demonstrates linear behavior to a certain extent and then shows nonlinear behavior. The ultimate linear behavior of concrete follows a general rule, according to which, if a six-dimensional space is considered with each of its dimensions representing a component of the stress tensor, there will be a procedure in this space called the yield level. The material displays linear behaviour in response to the increase of load in the places where the state of stress is located inside the mentioned procedure, and on the contrary, the material displays nonlinear behavior in response to the increase of load in the places where the state of stress is located outside this procedure.

Table 1. Characteristics of steel materials considering stress and strain (Ji et al., 2013).

Steel section	Modulus of Elasticity (MPa)	Poisson ratio	Plastic strain	Yield stress (MPa)
Beam box and column	2.1E+05	0.29	0-0.27	298.6-443.6
Shear wall sheet	2.1E+05	0.3	0-0.27	322.1-443.5
Bolts	2.0E+05	0.28	0-0.27	788.3-914.0

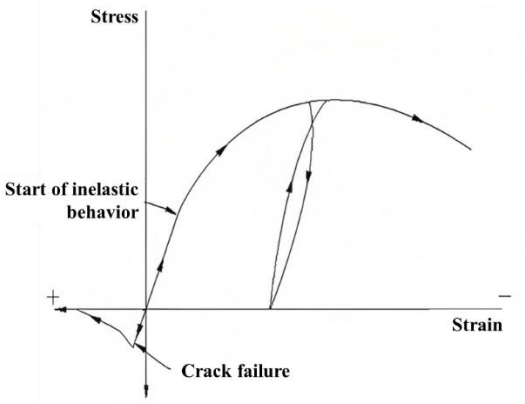

Figure 3. Stress-strain diagram of concrete.

To determine the level of yield, while various criteria have been proposed by researchers, in the present study, the Von Mises stress contour has been used. In addition, this study takes advantage of the default model available in ABAQUS, namely Concrete Damaged Plasticity (CDP), to model the behavior of concrete. CDP is a powerful model used for different loadings and expressing the behavior of concrete in pressure and tensile separately. The material model is capable of replicating the damage behavior with greater accuracy. To determine the trend of changes in the strength of concrete in pressure and tension, the yield function suggested by Lubliner in this model, corrected by (Chen et al., 2015) is used, as displayed in Eq. 1.

$$F\left(\bar{\sigma},\tilde{\varepsilon}^{pl}\right)\frac{1}{1-\alpha}\left(\bar{q}-3\alpha\bar{p}+\beta\left(\tilde{\varepsilon}^{pl}\right)\left\langle\hat{\bar{\sigma}}_{\max}\right\rangle-\gamma\left\langle-\hat{\bar{\sigma}}_{\max}\right\rangle\right)-\bar{\sigma}_c\left(\tilde{\varepsilon}^{pl}\right)\leq 0 \qquad (1)$$

In Eq. 1, effective stress is denoted by $\bar{\sigma}$ is determined when the damage parameter (d) is zero. Effective hydrostatic pressure and effective stress are $\bar{p}$ and $\bar{q}$ respectively and $\hat{\bar{\sigma}}_{\max}$ represent the maximum mean effective stress. Finally, α is a function of biaxial stress and compressive strength of concrete, calculated according to Eq. 2.

$$\alpha=\frac{f_b'-f_c'}{2f_b'-f_c'} \qquad (2)$$

The value of α varies between 0.08 and 0.12 and f_b'/f_c' ratio varies between 1.1 and 1.16. The β coefficient, which is also a function of the plastic strain tensor and α is calculated according to Eq. 3.

$$\beta\left(\tilde{\varepsilon}^{pl}\right)=\frac{\bar{\sigma}_c\left(\tilde{\varepsilon}_c^{pl}\right)}{\bar{\sigma}_t\left(\tilde{\varepsilon}_t^{pl}\right)}\left(1-\alpha\right)+\left(1+\alpha\right) \qquad (3)$$

The coefficient γ is also a function of the constant K_c, which controls the shape of the yield surface in deflection planes, and is used when $\hat{\bar{\sigma}}_{\max}$ is less than, or equal to zero. The flow potential function used in the CDP model is the Drucker-Prager hyperbolic function, defined in the space of hydrostatic pressure and Mises's deflection stress according to Eq. 4 (Epackachi et al., 2014).

$$G=\sqrt{\left(\chi f_t'\tan\psi\right)^2+\bar{q}^2}-\bar{p}\tan\psi \qquad (4)$$

In this equation, f_t' is the tensile strength of concrete or in other words, the cracking stress of concrete, which according to ACI-318, is considered equal to $0.62\sqrt{f_c'}$. Furthermore, the 28-day compressive strength of the standard cylindrical sample, denoted by f_c', is considered equal to 40 MPa (Ajimituhuo et al., 2018). Moreover, the eccentricity is denoted by χ the angle between the Von-Mises deflection stress and the hydrostatic stress, which is called the expansion angle and is denoted by ψ, varies between 15 and 45 degrees (Epackachi et al., 2014). Here, the value of G at high confinement pressure approaches zero and does not have much effect on the overall response, but if it is chosen to be too small, it causes divergence of the solution in the early stages (Mander et al., 1988, Nguyen, 2016). Based on the above, Table 2 displays the characteristics of the CDP model used for numerical simulation of concrete behavior in ABAQUS.

Table 2.CDP model specifications for simulating concrete behavior.

Poisson ratio	f_b'/f_c'	K_c	ψ	χ	Viscosity	Elastic modulus (MPa)	Specific mass (kg/mm^2)
0.17	1.16	0.67	0.36	0.1	0.00001	29725	2.5E-006

The stress-strain relationship is defined for modeling concrete materials in the CDP model according to Eq. 5.

$$\{\sigma\} = (1-d)[C]\{\varepsilon - \varepsilon^{pl}\} \qquad (5)$$

In Eq. 5, $\{\sigma\}$ and $\{\varepsilon\}$ are the stress and strain tensors of concrete, $\{\varepsilon^{pl}\}$ is the plastic strain tensor and [C] is the elastic stiffness matrix. d is the scalar parameter of concrete damage, which is applied to the hardness of the concrete due to the damage caused. It varies between zero for undamaged concrete and 1 for wholly damaged concrete (Mander et al., 1988). Since steel plates surround the concrete and lacks tightly-closed horizontal and vertical reinforcements, the present study takes advantage of the stress-strain model available for the concrete core with composite rectangular columns. In this model, the confinement caused by the concrete cover only affects the ductility of the concrete and has no role in increasing the strength of the concrete. This follows the results of the experiments conducted in literature. The general trend of the stress-strain diagram in the model is displayed in Fig. 4.

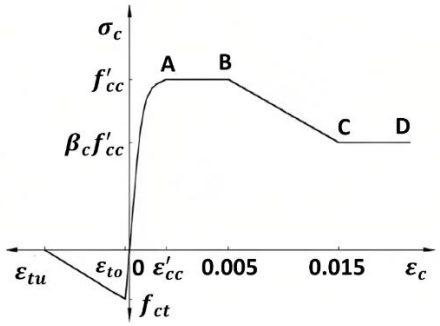

Figure 4. Model used to determine the stress-strain diagram of concrete (Committee, 2008).

In the OA area, the stress-strain relationship of concrete is based on the relationships presented by Mender et al. (Eqs. 6, 7 and 8).

$$\sigma_c = \frac{f'_{cc}\lambda(\varepsilon/\varepsilon'_{cc})}{\lambda - 1 + (\varepsilon/\varepsilon'_{cc})^{\lambda}} \qquad (6)$$

$$\lambda = \frac{E_c}{E_c + (f'_{cc}/\varepsilon'_{cc})} \qquad (7)$$

$$\varepsilon'_{cc} = \begin{cases} 0.002 & f'_c \le 28MPa \\ 0.002 + \dfrac{f'_c - 28}{54000} & 28 < f'_c \le 82MPa \\ 0.003 & f'_c > 82MPa \end{cases} \quad (8)$$

In Eqs. 6,7 and 8, σ_c and ε_c are the compressive stress and strain of concrete, respectively; f'_{cc} is the effective compressive strength of concrete due to enclosure, ε'_{cc} its corresponding strain and E_c is the elasticity modulus of the concrete. The value of f'_{cc} depends on the dimensions of the steel coating, the quality of the concrete and the amount of loading, and can be calculated according to Eq. 9.

$$\begin{aligned} f'_{cc} &= \lambda_c f'_c \\ \lambda_c &= 1.85 D_c^{-0.135} \qquad 0.85 \le \lambda_c \le 1 \end{aligned} \quad (9)$$

In Eq. 9, D_c is the larger value of two expressions (*D*-2*t*) and (*B*-2*t*), in which, *D* and *B* are the length and width of the rectangular section of the steel cover and *t* is its thickness.
The β_c coefficient is also obtained according to Eq. 10.

$$\beta_c = \begin{cases} 1 & D/t \le 24 \\ 1.5 + D/48t & 24 < D/t \le 48 \\ 0.5 & D/t > 48 \end{cases} \quad (10)$$

The relationships of the segments AB, BC and CD of the stress-strain diagram of Fig. 4 are described in Eq. 11.

$$\sigma_c = \begin{cases} f'_{cc} & \varepsilon'_{cc} < \varepsilon_c \le 0.005 \\ \beta_c f'_{cc} + 100\left(0.015 - \varepsilon_c\right)\left(f'_{cc} - \beta_c f'_{cc}\right) & 0.005 < \varepsilon_c \le 0.015 \\ \beta_c f'_{cc} & \varepsilon_c > 0.015 \end{cases} \quad (11)$$

2.5. Loading and validation

Fig. 5a shows the test setup and the composite shear wall sample placement in the loading frame. To apply the loading, a vertical load was first applied to the sample and maintained continuously throughout the test. Subsequently, as displayed in Fig. 5b, one-way cyclic lateral loading was applied quasi-statically by the actuator mounted horizontally on the wall.

In each cycle loading, a pressure (positive charge) and stress (negative charge) were first applied. Similar loading mechanism was utilized in the numerical model. To load the model, a displacement history was used for the upper beam, as shown in Fig. 5c. Fig. 5c shows the buckling results created in the studied shear wall regarding the amount of stress produced. Due to the one-sided lateral loading applied to the experimental model, buckling of steel plates occurs on one side of the wall, specifically at its compressive toe.

Fig. 6 compares the distribution of tensile and compressive buckling damage of steel plates reported in the experiment with those obtained from the numerical model. Fig. 7 shows the results of the capacity curve (force-displacement) obtained from the pushover analysis of the FE model, compared to the experimental model. The table also shows a comparison of numerical modelling results and experimental results. The displacement value equal to 0.85 of maximum strength was considered the final displacement of the wall.

As evident from the review of Fig. 7 and Table 3, the results obtained from FE analysis are consistent with the experimental results. It is important to note that, though the experimental and numerical results closely corelate, there is a deviation of more

than 5% in the region of 20-30mm displacement. This can be attributed to the fact that numerical model does not reproduce the tightly packed condition of steel plate around the concrete and this condition severely affects the effective compressive strength behavior of the concrete. Also, the numerical material model only determined the ductility of concrete and has no role in strength consideration due to confinement. This leads to lower lateral load prediction as the displacement increases.

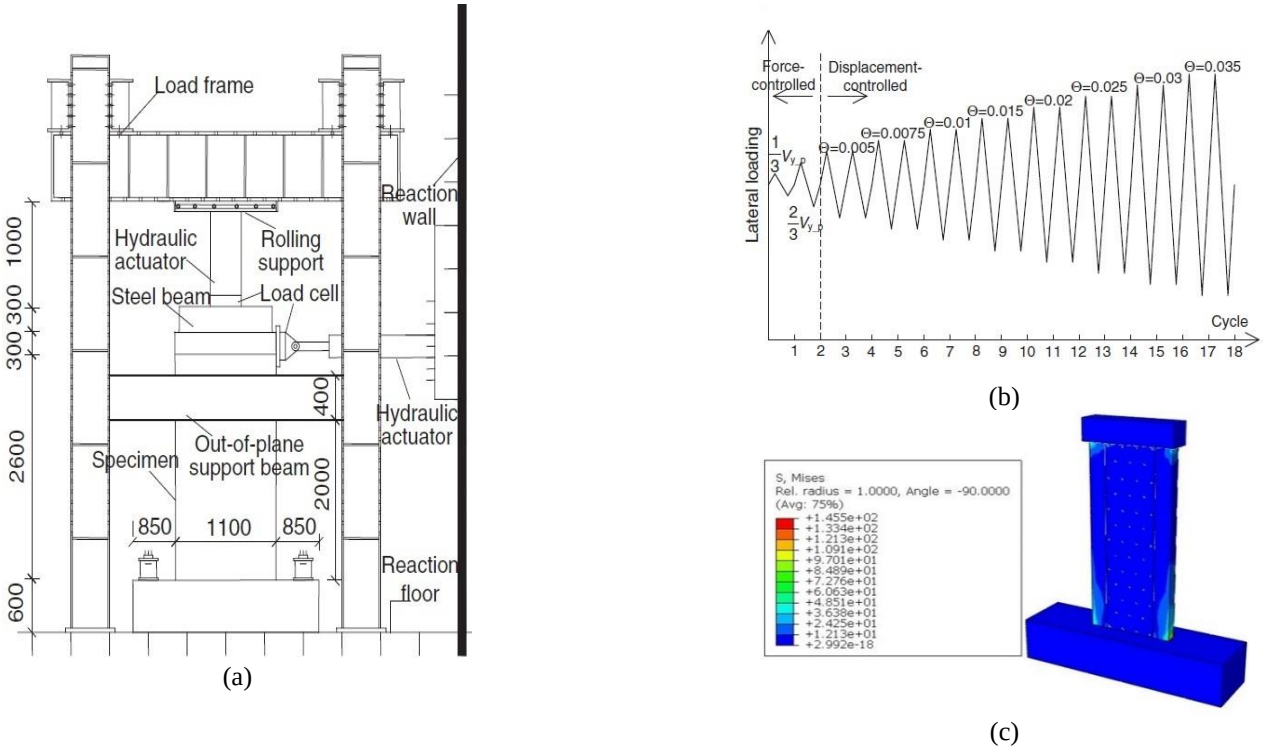

Figure 5. a) Experimental model set-up, b) loading history applied to the wall, c) buckling created in the wall.

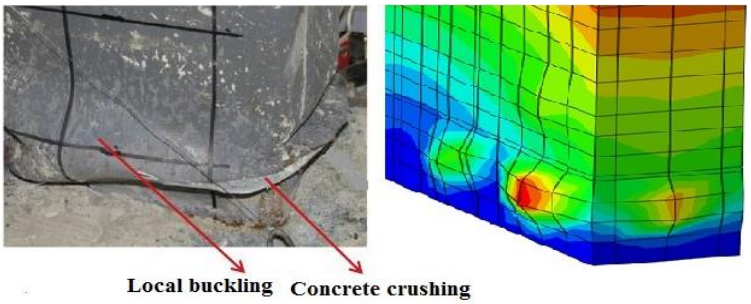

Figure 6. Comparison of results obtained from the experimental model and numerical modelling of the composite shear wall, buckling pattern of steel plate in wall.

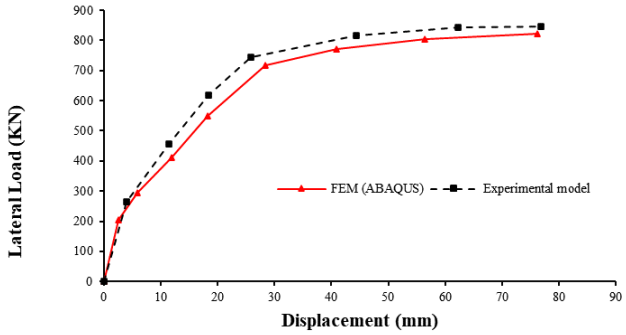

Figure 7. Load- displacement curve.

Table 3. Comparison of experimental values and numerical modelling for the behavior of the studied sample.

Specimen	Lateral stiffness (kN/mm)	Surrender displacement (mm)	Surrender resistance (kN)	Deformation capacity (mm)	Maximum resistance (kN)	Ductility coefficient
Experimental model	72.95	16.7	744.98	52.9	846.98	2.98
Numerical model	78.25	16.1	715.91	50.15	823.71	3.11
Percentage difference	7.3	-3.6	-3.9	-5.2	-2.7	4.4

2.6. Blast loading

In general, the blast loading applied in the previously studied samples have not been according to any special protocol. Therefore, in this study, compressive and incremental loadings were applied at a constant rate with a time step of 0.001 seconds and until the maximum compressive load to the model was achieved. For blast loading, it is necessary to accurately determine the two fundamental parameters, including the amount of charge and its distance from the structure. Depending on the level of blast hazard, different pressures are assumed to be applied to the structure. Generally, blast loading depends on two parameters, namely, time and place. In this research, to simplify and reduce the computer simulation time, the spatial dependence of the load in the models is disregarded, and only the temporal distribution of the load is discussed. In other words, the distribution of blast pressure is applied on the surface of the composite shear wall in the form of a uniform pressure that is a function of time. This can be accepted by referring to the blast code of the American Steel Structures Association (AISC). According to this standard, if the distance from the blast site to the structure is more than half of the smallest dimension of the structure, it can be safely assumed that the pressure on the shear wall is uniform.

The main parameters of the blast depend on two independent parts, namely the amount of energy released during the blast and the distance between the blast's centre and the blast wave's location. The destructive power of an explosion is calculated based on these two mentioned factors. (Goel & Matsagar, 2014) used Eq. 12 to calculate the maximum pressure due to blast load (p_{so}) (Liang, 2009).

$$p_{so} = 6784\frac{w}{R^3} + 93\left(\frac{w}{R^3}\right)^{0.5} \quad (12)$$

In the equation above, w is the weight of the equivalent blasts in terms of the of TNT weight, and R is the distance of the effect of the blasts.

According to the FEMA428 standard, loads of about 35 to 80 kg of charge at a distance of less than 15 meters cause destruction of a structure. Based on the initial numerical modeling, this paper concluded that the mentioned equivalent load at intervals of less than 10 meters causes large damage to the composite shear wall. Therefore, in this study, the design load was considered the blast load equivalent to 50 kg of TNT at a distance less than 10 m of the composite shear wall. As a result, by calculating the blast load using Eq. 12, the compressive load caused by this blast was determined to equal 36 MPa. It

should be noted that the pressure was applied to the wall in the form of a trapezoid during the total time of 0.02 seconds. Table 4 shows the load time range and pressure on the model during different time steps.

Table 4. Time range of compressive loading due to blast on composite shear wall model

Pressure (MPa)	Time period (seconds)
0	0.000
36	0.001
36	0.01
0	0.02

2.7. Parametric analysis

After validating the composite shear wall model based on the numerical method in ABAQUS, nonlinear analysis was used to evaluate the performance of this system while it was reinforced with FRP sheets and subjected to the effect of blast loading. Based on this, 17 numerical composite shear wall models reinforced with FRP sheets were simulated and analyzed. Among these, two samples were modelled to determine the effect of the presence of FRP sheets, three samples to determine the impact of blast load intensity, three samples to determine the effect of FRP sheet material, three samples to determine the effect of sheet thickness and three samples to assess the effect of FRP sheet spacing.

In addition, three samples were simulated to measure the effect of steel plate thickness. Two samples were to investigate the effect of steel plate cross-sectional shape, and three samples were to determine the effect of concrete compressive strength. To analyze the results, the displacement of the sheet's middle and the support reaction force's equivalent force were determined. The obtained force-displacement diagram was compared to evaluate the performance of the composite shear wall reinforced with FRP sheets. It is essential to highlight that the outputs obtained from the software analysis are utilized to assess the performance of the composite shear wall. These outputs include stress, strain, and displacement contours, as well as displacement values, inner energy, and strain energy over time. They provide valuable insights into the behaviour of the simulated composite shear wall under the influence of blast loads in various states. Based on these outputs, the data and results are compared.

3. Results and discussions

This section evaluates the results of numerical modeling based on parametric studies. For this purpose, the effect of FRP sheets in the composite shear wall and the effect of blast load intensity on wall performance were examined. Then, the effect of FRP sheet type, thickness and spacing of sheets on the behaviour of the wall under blast load was assessed. Finally, the effect of steel plate thickness and cross-sectional shape in both without-hole and with-hole modes and the effect of compressive strength of concrete were studied.

3.1. The effect of the presence of FRP sheets

In this section, the effect of adding an FRP sheet on the performance of the shear wall under the effect of blast load was investigated. Fig. 8 displays the stress and displacement contours created in the composite shear wall in two modes without and with FRP sheet. As can be observed, using FRP sheets in the composite shear wall has increased the stress absorption due to the increased load transfer capacity and high energy dissipation by the polymer fibers. Fig. 9a shows the results of the composite shear wall displacement in terms of time in two different modes without and with the FRP sheet. The results confirm that using the FRP sheet has reduced the wall displacement by 18.5%.

This is because the use of FRP creates cohesion in the wall components and prevents the local collapse of the wall under blast to some extent, and also has partially reduced the movement outside the wall plate. This effect delays the local rupture of the wall and is the main reason for the reduced displacement of the composite wall, thus resisting the blast load. Figs. 9b and c show the internal and strain diagrams of the composite wall under the effect of blast load in two different modes without and with FRP sheet, respectively. As it is clear from the results displayed in Fig. 10b, the inner energy of the wall in the two

cases, with and without FRP sheet, is equal to 132511 and 132118 kJ, respectively, and FRP sheets increase the inner energy of the wall. The main reason for this behavior is the energy dissipation by FRP sheets in the system. The result is inversely related to the changes in strain energy stored in the wall in both cases, with and without FRP amplification, and using FRP has reduced the strain energy of the wall by about 50%.

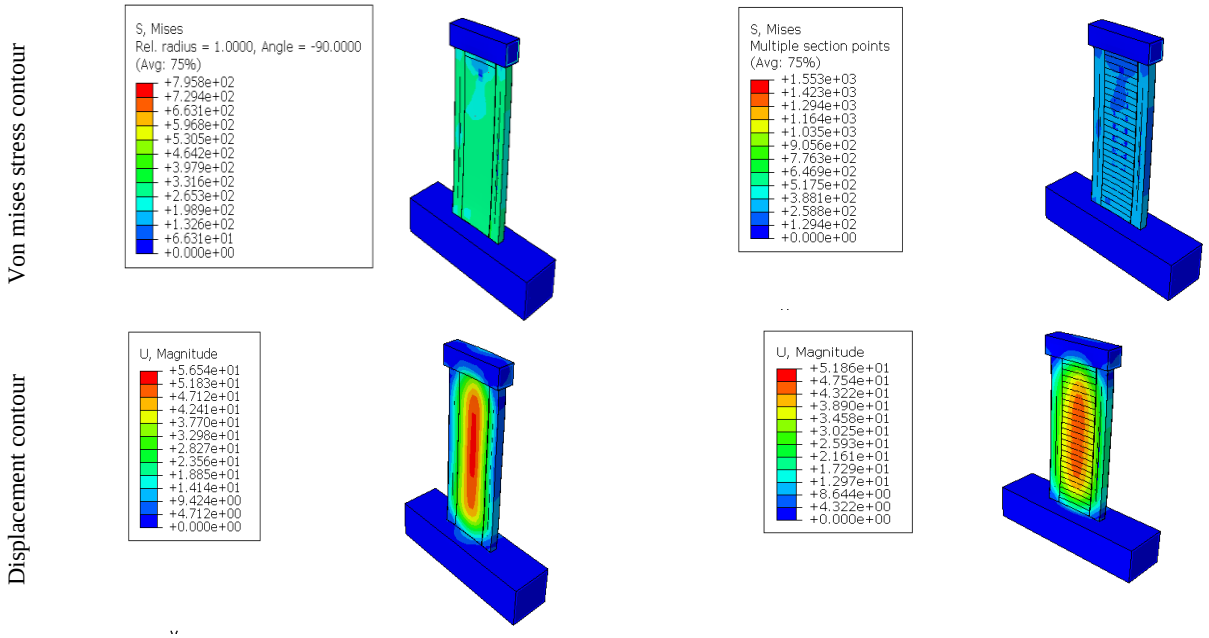

(a) Without FRP (a) With FRP

Figure 8. The effect of FRP sheet on stress contour and displacement of composite shear wall under blast load.

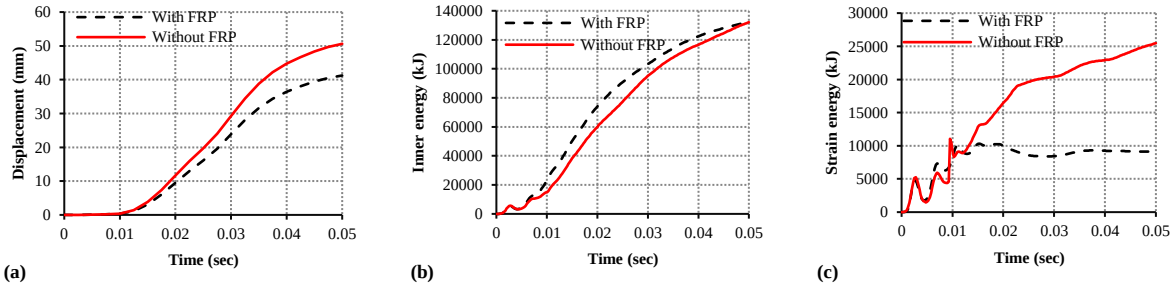

Figure 9. Comparison diagram of displacement and stored energy of composite wall without and with FRP sheet under the effect of blast load, (a) displacement, (b) inner energy, (c) strain energy.

3.2. Impact of blast intensity

In this section, the results related to the effect of blast load intensity on the performance of FRP sheets in composite shear walls are evaluated. To investigate the effect of the blast load intensity, three TNT charges, equivalent to 10, 40, 60 MPa were considered as the blast of minimum, medium and maximum size, respectively. Fig. 10 shows the results for Von Mises stress contours and the displacement created in the composite shear wall for different blast intensities. As observed, with the increasing intensity of the blast, the stresses and displacements created in the wall also increased.

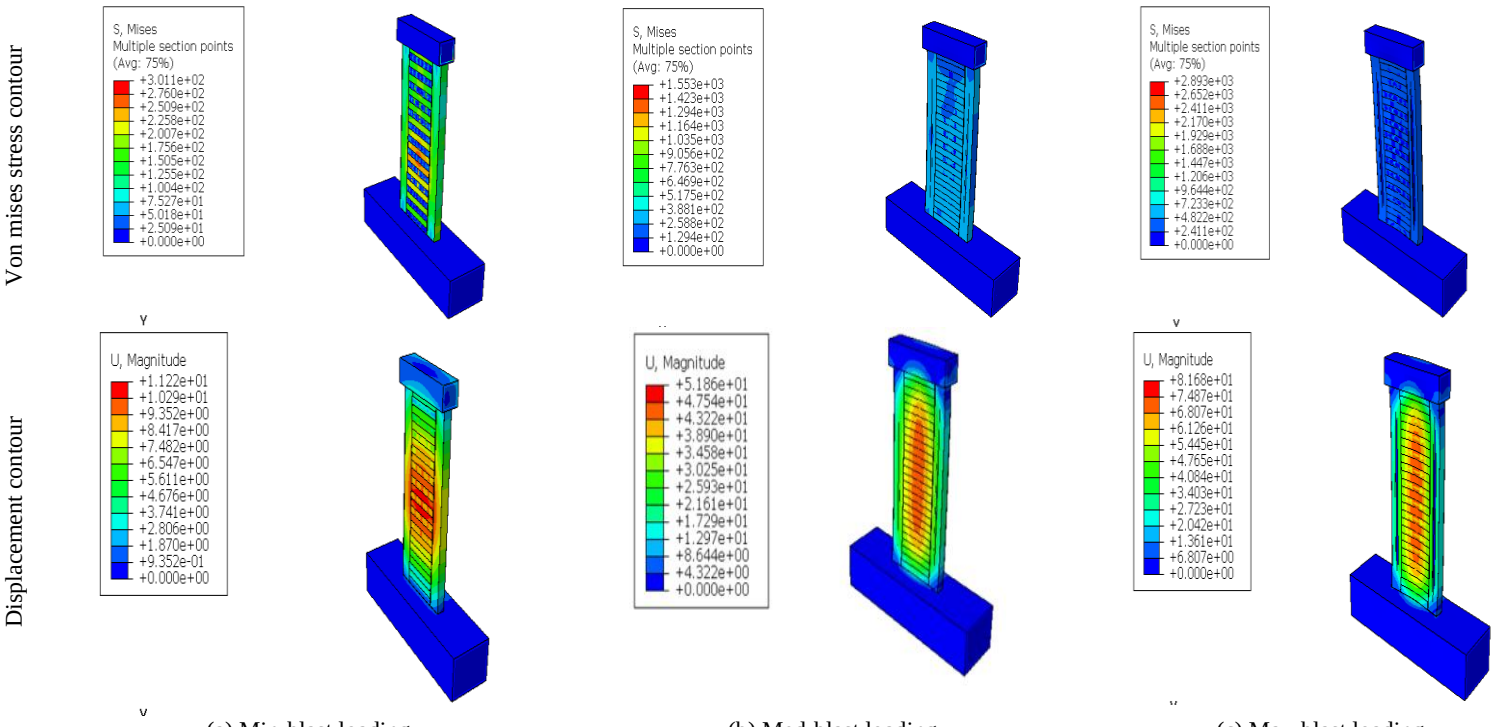

(a) Min-blast loading (b) Med-blast loading (c) Max-blast loading

Figure 10. Comparison of stress contours and displacement of composite shear wall with FRP sheets under different blast intensities.

Fig. 11a shows the results of the displacement of the FRP-reinforced wall for different blast intensities. It is evident that by increasing the intensity of the blast load, the displacement of the wall increased from 10.05 mm to 62.94 mm. This signifies an increase of 84% in the displacement when the blast load is increased from 10MPa to 60MPa. Fig 11b demonstrates the comparative results related to the effect of blast intensity on the inner energy of the composite shear wall. It is observed that with increasing the intensity of the blast, the inner energy of the wall has reached from 8935 kJ to 297397 kJ. In addition, the strain energy diagram of the composite shear wall under the effect of blast load with different intensities is displayed in Fig 11c, showing that the strain energy increased from 2474 kJ to 21107 kJ with the increase of blast intensity.

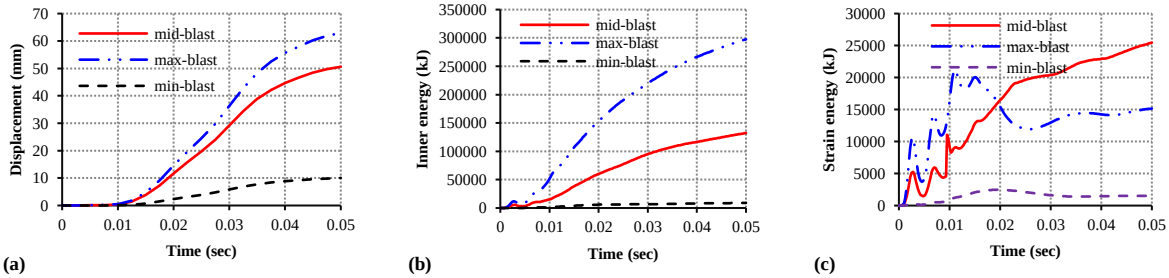

(a) (b) (c)

Figure 11. Comparison diagram of displacement and stored energy of composite shear wall with FRP sheets under different blast intensities, (a) displacement, (b) inner energy, (c) strain energy.

3.3. The effect of the material of FRP sheets

The results of the effect of carbon fiber-reinforced polymer (CFRP), aramid fiber-reinforced polymer (AFRP) and glass fiber-reinforced polymer (GFRP) on the stresses, strains and displacements created in the composite shear wall with FRP strip under blast load are shown in Fig. 12. Based on the results displayed in Fig. 12a, it can be seen that the use of carbon fibers results in better performance regarding absorption of stress, compared to other fibers. While, GFRP have the weakest

performance in stress absorption. Compared to other fibers, this effect of carbon fibers is due to their tensile strength and low density. The results of the FRP sheet material on the strains created in the wall are demonstrated in Fig. 12b. The results suggest that the highest amount of strain was created in GFRP and the lowest amount of strain was created in CFRP, which is due to the low tensile strength of glass fiber when compared to that of carbon fiber.

According to Fig. 12c, it is evident that the maximum displacement of the wall due to the blast load occurs in the center of the wall, and the displacement in the wall with CFRP sheets, is less than the displacement in the wall with another polymer fibers. The main reason for this behavior is the high stiffness and elasticity modulus of CFRP sheets, compared to other fibers, which show more resistance and reduce the displacement created in the wall in the face of blast load.

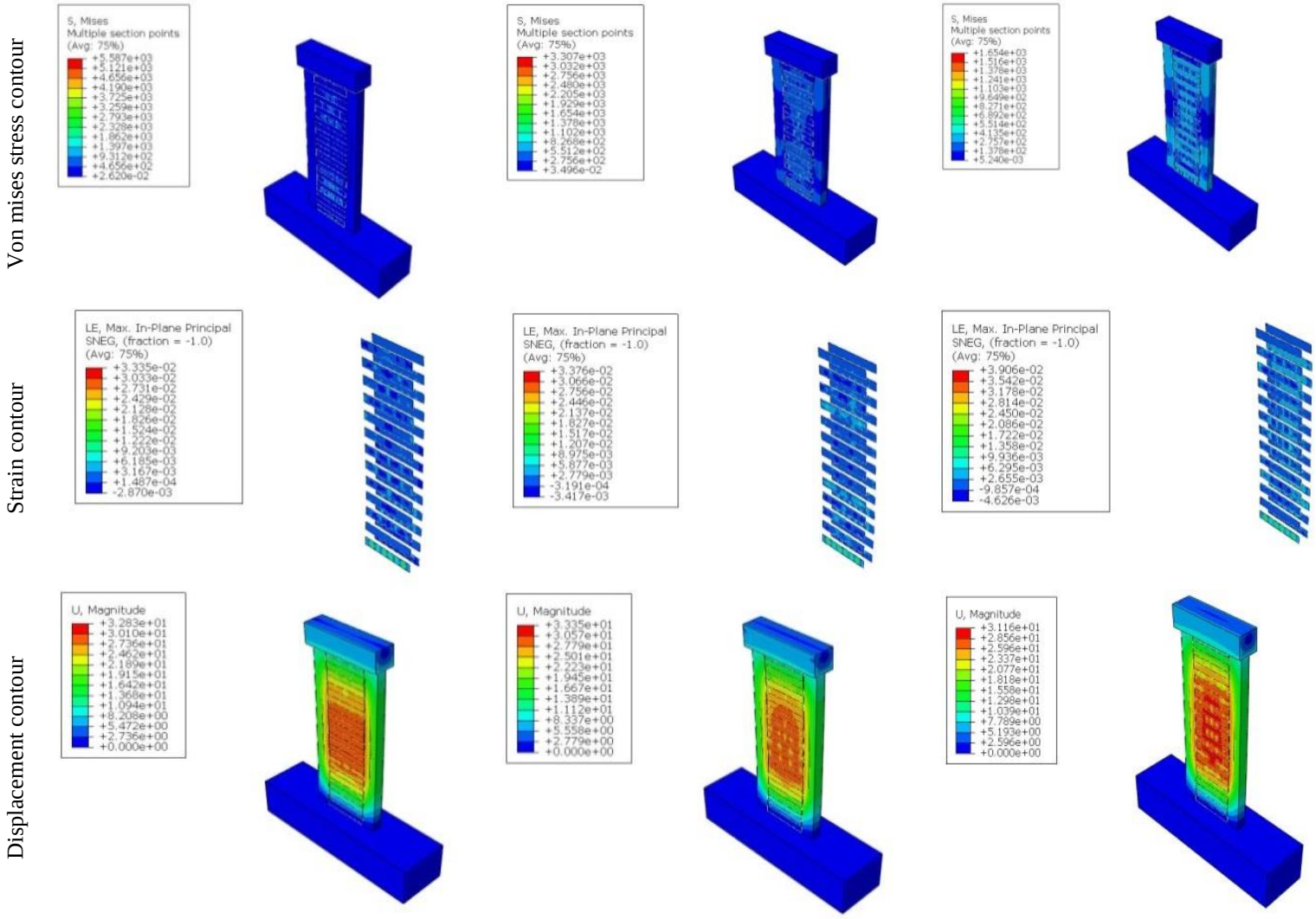

(a) CFRP (b) AFRP (c) GFRP

Figure 12. Comparison of the effect of FRP sheet material on (a) stress contours, (b) strain and (c) displacement of composite shear wall with FRP sheets under blast load.

Fig. 13a shows the effect of the material of FRP sheets on the results of displacement in terms of time. The results indicate that, as previously stated, the displacement created in the wall with CFRP sheets is less than the displacement created in the wall with other polymer fibers. Figs. 13b and c show the inner energy and strain diagrams of the composite shear wall with CFRP, AFRP and GFRP fibers under blast load, respectively.

The results show that the inner energy generated and also the energy loss in the shear wall of carbon fibre reinforced composite (CFRP) is less when compared to other fibers. This indicates the superior performance of CFRP sheets compared to that of other fibers. In contradiction to displacement and internal energy results, the amount of strain energy generated in the CFRP wall is higher than in other fibers. Also, the maximum peak strain energy of 27075kJ was achieved in CFRP laminate at 0.026 s, while the minimum peak strain energy of 21055kJ was achieved by AFRP laminates at 0.034s. This behavior can be attributed to CFRP being brittle compared to other fibers.

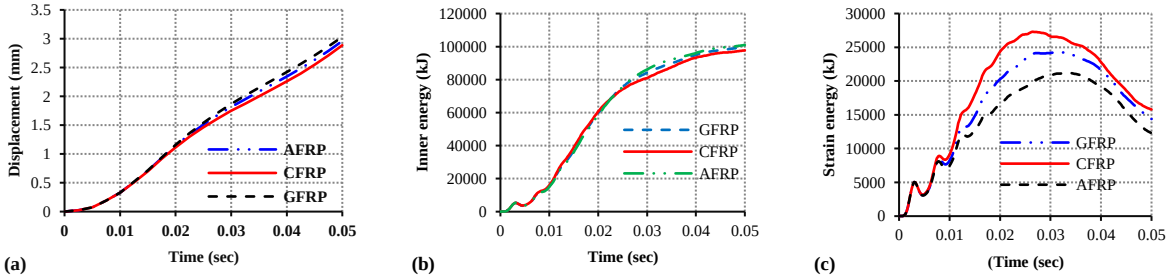

Figure 13. Comparison diagram of the effect of FRP sheet material on displacement and stored energy of FRP sheet reinforced composite shear under blasting, a) displacement, b) inner energy, c) strain energy.

3.4. Effect of FRP sheet thickness

The results of the effect of the thickness (t) of FRP sheets on the stresses, strains and displacements created in the composite shear wall with FRP strip under the blast load are shown in Fig. 14. Based on the results in Fig. 14a and b, it can be seen that by increasing the thickness of FRP sheets from 1 to 5 mm, the stresses and strains created in the composite shear wall are reduced. Also, due to stress absorption, polymer fiber has prevented a higher concentration of local stress in the composite's shear wall. This effect increases by increasing the thickness of polymer fiber. The main reason for this is the increase in final resistance due to the increase in the thickness of the FRP sheet. In addition, the reason for the reduction of wall strains is the increase in the final strength of the fiber due to the increase in the thickness of the fiber.

Von mises stress contour

Strain contour

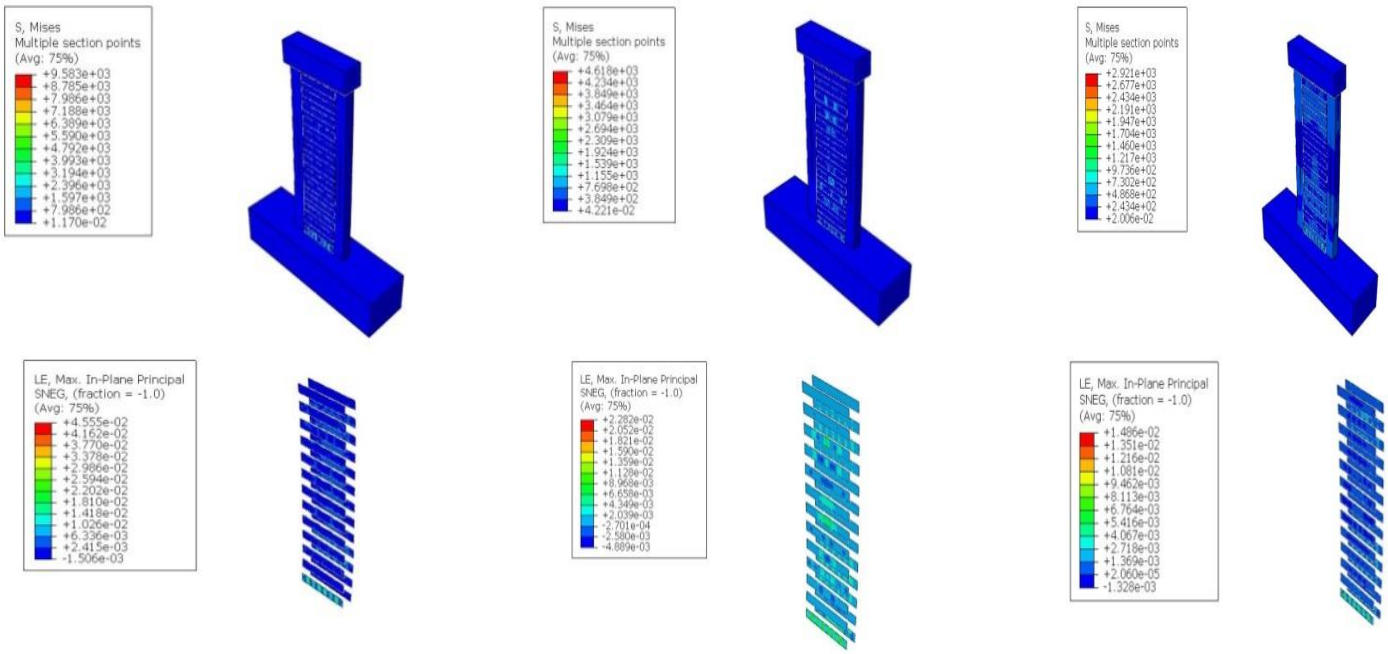

Displacement contour

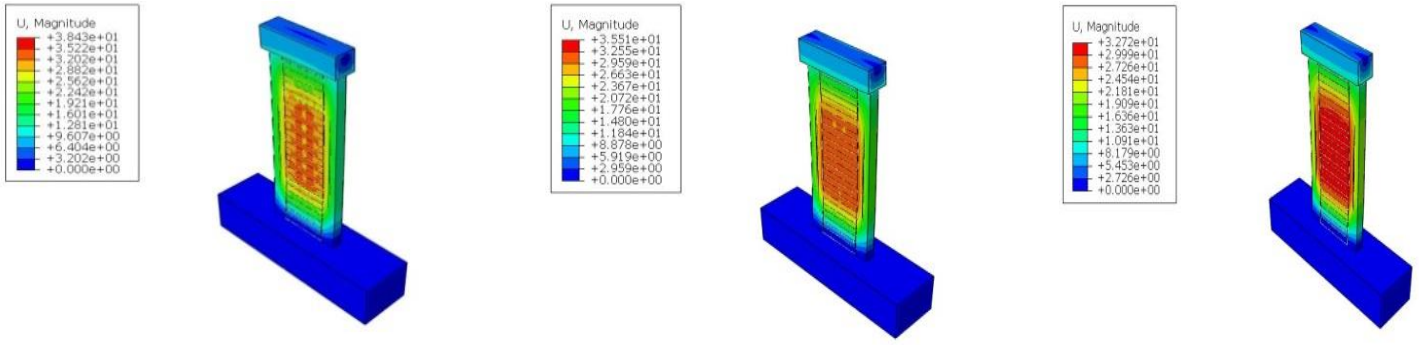

(a) t = 1 mm (b) t = 3 mm (c) t = 5 mm

Figure 14. Comparison of the effect of FRP sheet thickness on (a) stress contours, (b) strain and (c) displacement of composite shear wall with FRP sheets under blast load.

Fig. 15a displays the effect of FRP sheet thickness on composite shear wall displacement in terms of time. The results show that by increasing the thickness of polymer fibers from 1 to 5 mm, the displacement of the composite shear wall is reduced, which is due to the increase in final strength, resulting from the increasing thickness of polymer fibers. Fig. 15b and c show the internal and strain diagrams of the composite wall under the effect of blast load for different thicknesses of FRP sheet, respectively. The results suggest that with increasing the thickness of polymer fibers, the inner energy generated in the composite shear wall decreases, while its amount of strain energy increases by 41% as compared to 1mm thick FRP. The main reason for this behavior is the increase in yield stress in the FRP sheet, which has increased the final strength of the FRP sheet.

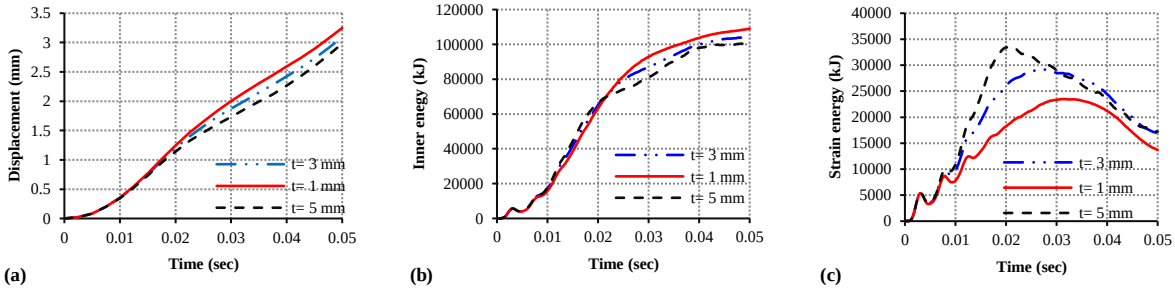

(a) (b) (c)

Figure 15. Comparison diagram of the effect of FRP sheet thickness on displacement and stored energy of composite shear wall with FRP sheet under blasting, a) displacement, b) inner energy, c) strain energy.

3.5. The effect of distance between FRP sheets

In this section, the results of the effect of distance (s) between FRP sheets on the stresses, strains and displacements created in the composite shear wall with FRP strip under blast load are compared. As it is evident from Fig. 16a, by increasing the vertical distance between the FRP sheets, the stress borne by the shear wall decreases due to the decrease in the number of fibers, which is in turn, due to the increase in the distance between them. In addition, the results of Fig. 16b show that as the distance between the FRP sheets increases, the strains created in the fibers first increase and then decrease. The main reason for this is the effect of fiber distance on stress absorption: the greater the distance, the lower the performance of polymer fibers in increasing the ductility of the composite shear wall.

Fig. 16c depicts the displacement contours created in the wall for different distances of FRP sheets. Based on the obtained results, it is observed that by increasing the distance between FRP sheets, the displacement created in the composite shear wall is reduced due to the reduction in the number of sheets and thus the reduction of their final strength. Also, the highest amount of displacement in the composite shear wall is in the middle of the wall, which is due to the increased stress concentration in this area of the composite shear wall. Fig. 17a displays the results of the trend of the displacement changes of the wall in terms of time against the blast load. In addition, the results of inner energy and strain energy generated in the composite

shear wall for different distances of FRP sheets suggest that with increasing distance, the inner energy increases and the strain energy decreases. The reason for this behavior is the decrease in the final strength of the wall due to the reduction in the number of polymer sheets.

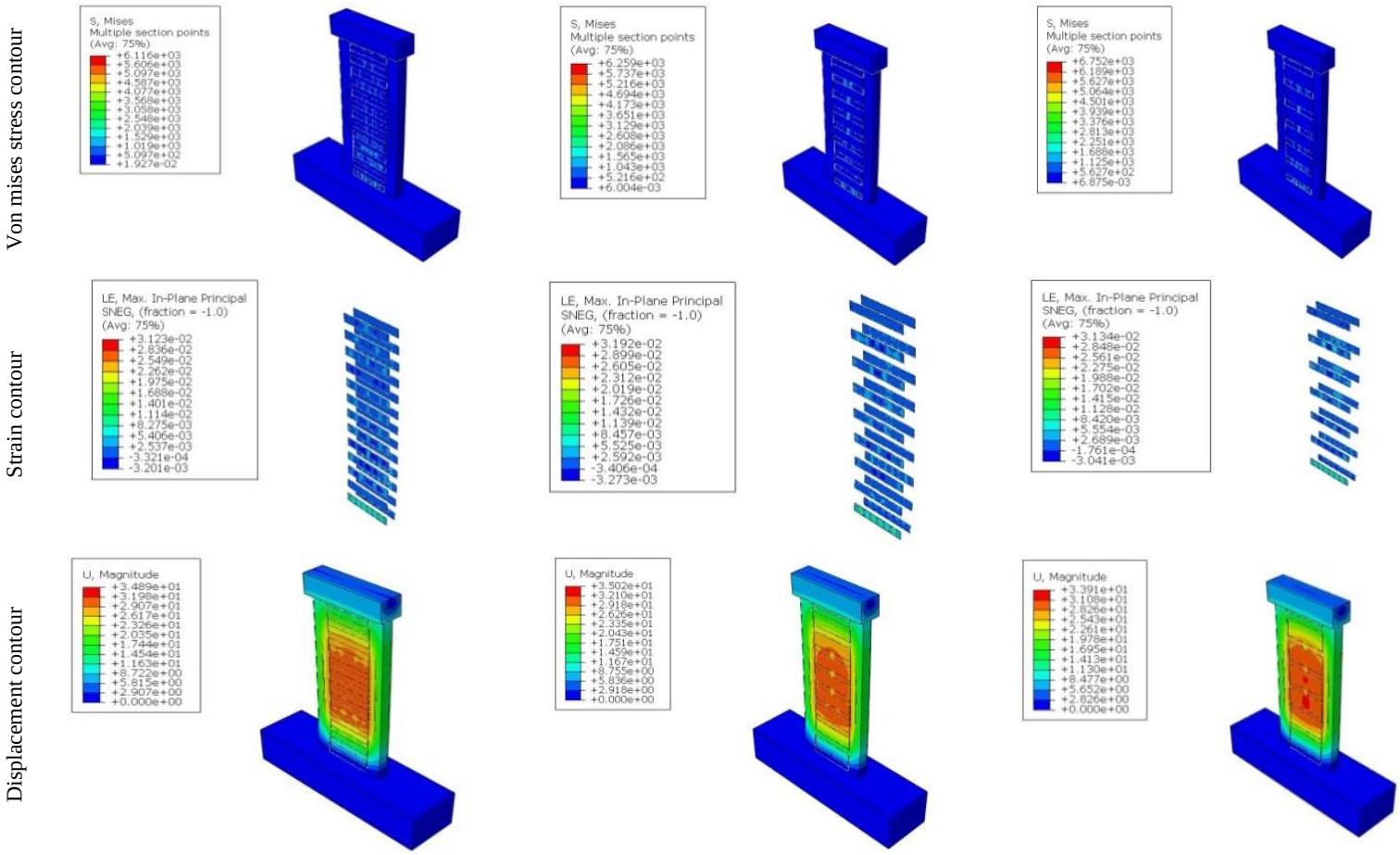

(a) S = 100 mm (b) S = 200 mm (c) S = 300 mm

Figure 16. Comparison of the effect of distance between FRP sheets on (a) stress contours, (b) strain and (c) displacement of FRP composite shear wall under blast load.

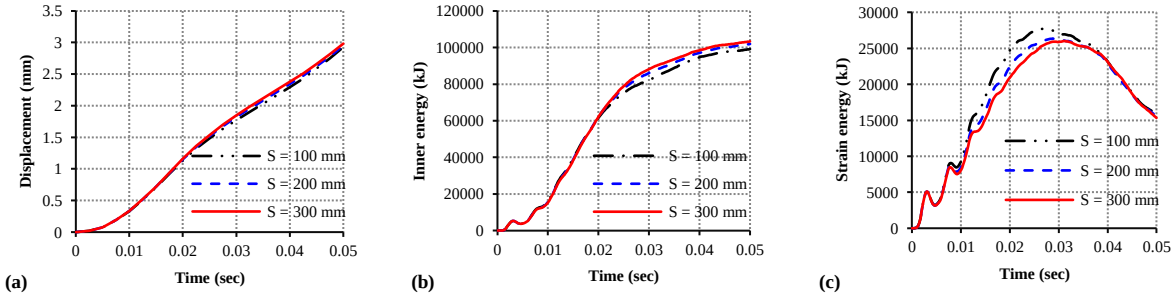

Figure 17. Comparison diagram of the effect of distance between FRP sheets on displacement and stored energy of a composite shear wall with FRP sheet under the effect of blast, a) displacement, b) inner energy, c) strain energy.

3.6. Effect of steel plate thickness

Fig. 18 shows the results of the effect of steel plate thickness (tP) on the stresses, strains and displacements created in the composite shear wall with FRP strip, under blast load. According to the results in Figs. 18a, b and c, by increasing the thickness of the steel plate to 7 mm, the stresses, strains and displacements created in the wall all saw a significant decrease initially, and then, with increasing the thickness of the steel plate, the values of these parameters increased. This finding indicates the effectiveness of increasing the thickness of the steel plate to a certain extent, exceeding which, in practice will not improve the performance of the composite shear wall.

Accordingly, the effective thickness of the steel plate for the best performance of the composite shear wall system under the effect of blast load is less than 7 mm, as confirmed in Fig. 19a. The results of inner energy and strain energy generated in the composite shear wall for different values of steel plate thickness, as displayed in Figs 19b and c, respectively, suggest that with increasing the thickness of steel plate, the energy experiences similar changes as in the stress contours: an initial decrease, followed by an increase. These results indicate the improvement of the performance of the composite shear wall by increasing the thickness of the steel plate to a certain extent (tP = 7 mm) under the blast load.

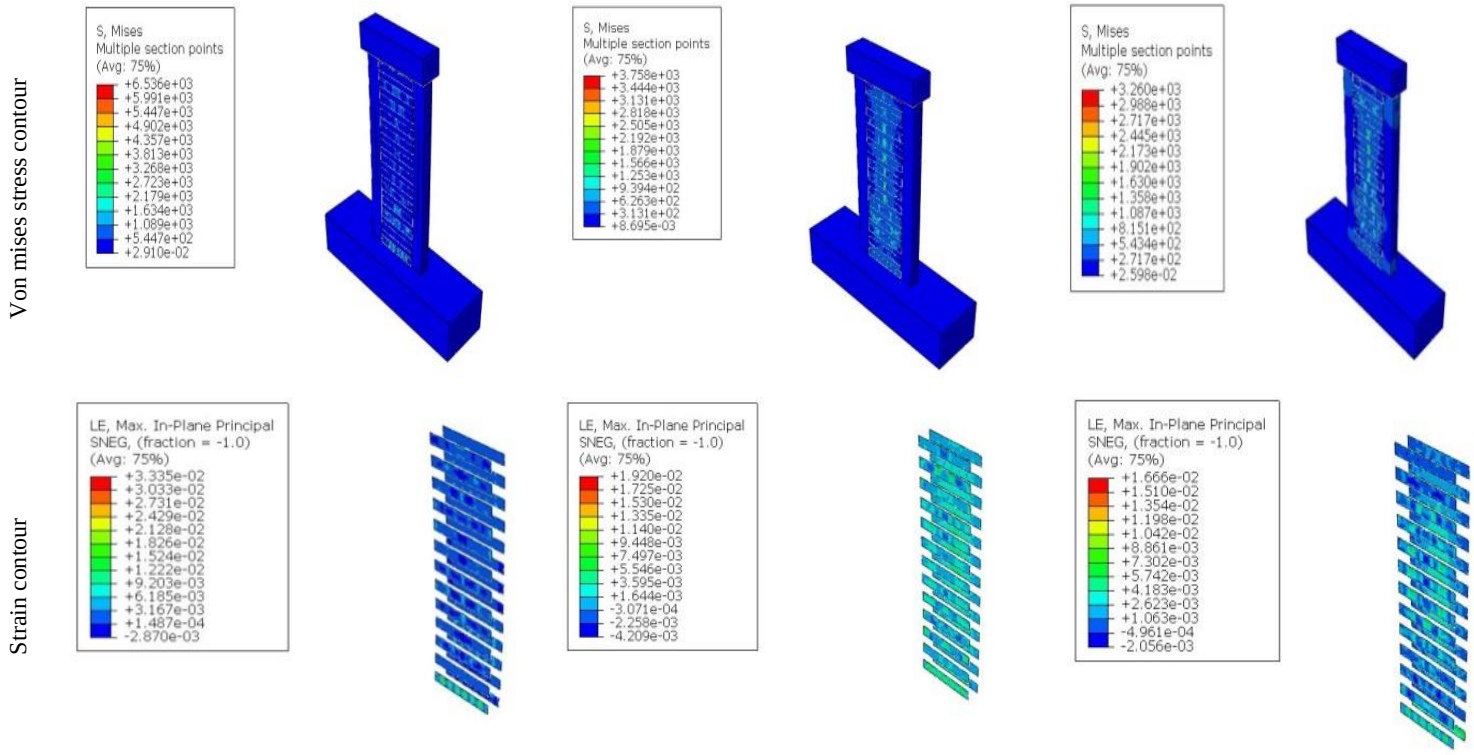

Displacement contour

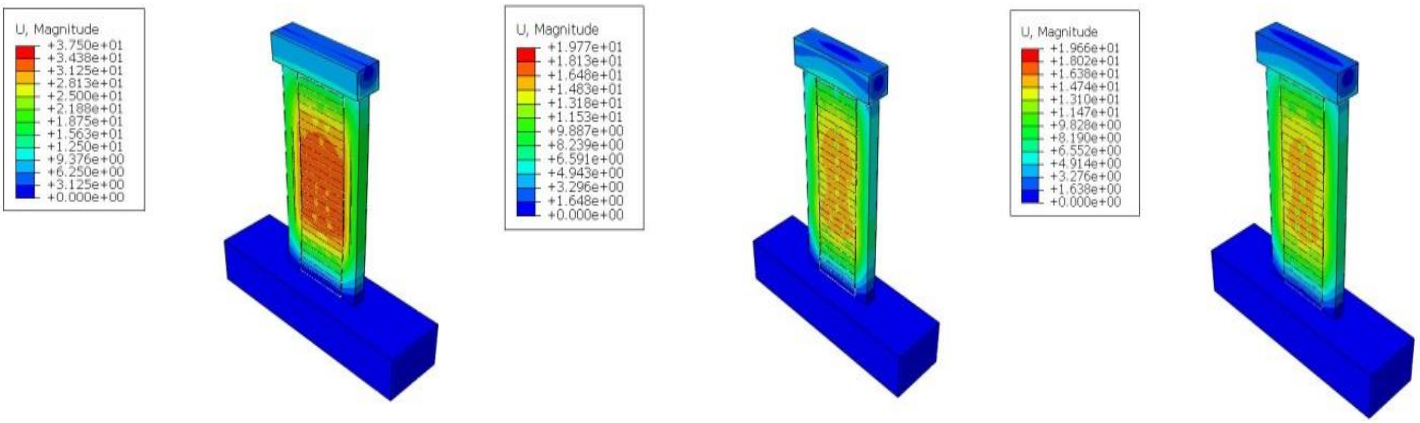

(a) t_P = 3 mm (b) t_P = 5 mm (c) t_P = 7 mm

Figure 18. Comparison of the effect of steel plate thickness on a) stress, b) strain and c) displacement of composite shear wall with FRP sheets under blast load.

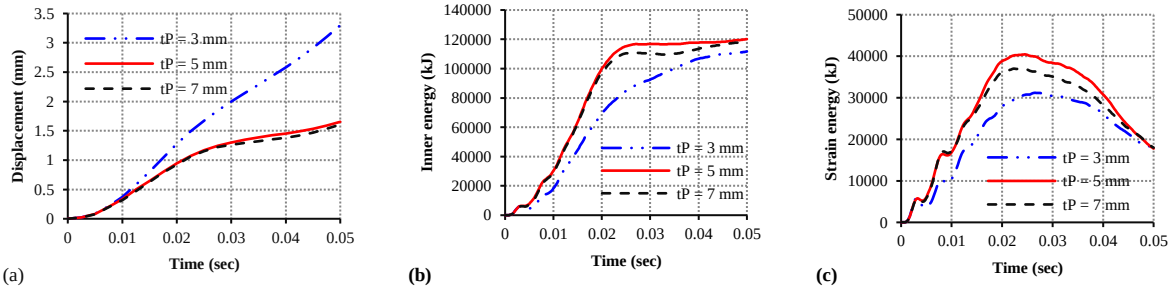

(a) (b) (c)

Figure 19. Comparison of the effect of steel plate thickness on displacement and stored energy of a composite shear wall with FRP sheet under the effect of blast, a) displacement, b) inner energy, c) strain energy.

3.7. The effect of cross section of steel plate

In this section, the effect of the cross-sectional shape of the steel plate on the performance of a composite wall with FRP strip under the effect of blast load is investigated. Figs. 20a, b and c show the results of stress, strain and displacement contours created in the composite shear wall in two different states of without-holes and with-holes steel plates, respectively. As it is evident, the stresses, strains and displacements created in the wall with with-holes steel plate are higher by 42%, compared to those in the without-holes sheet. The reason for this behavior is the decrease in the strength of the with-holes steel plate due to the presence of holes in the sheet.

Fig. 21a shows the results of displacement in terms of time for the composite shear wall in two different modes of the composite shear wall with a with-holes sheet and with a without-holes sheet. The results confirm that the displacement of the composite shear wall with the with-holes sheet is more than that with the without-holes sheet. The reason for this is the reduction in the strength of the with-holes steel plate due to the presence of holes and consequently, the reduction of the performance of the composite shear wall. Figs. 21b and c depict the inner energy and strain diagrams of the composite wall under the effect of blast load in two different states of with-holes and without-holes steel plates, respectively. The results suggest that the perforation of the steel plate increases the inner energy and on the other hand, has no effect on the strain energy of the wall.

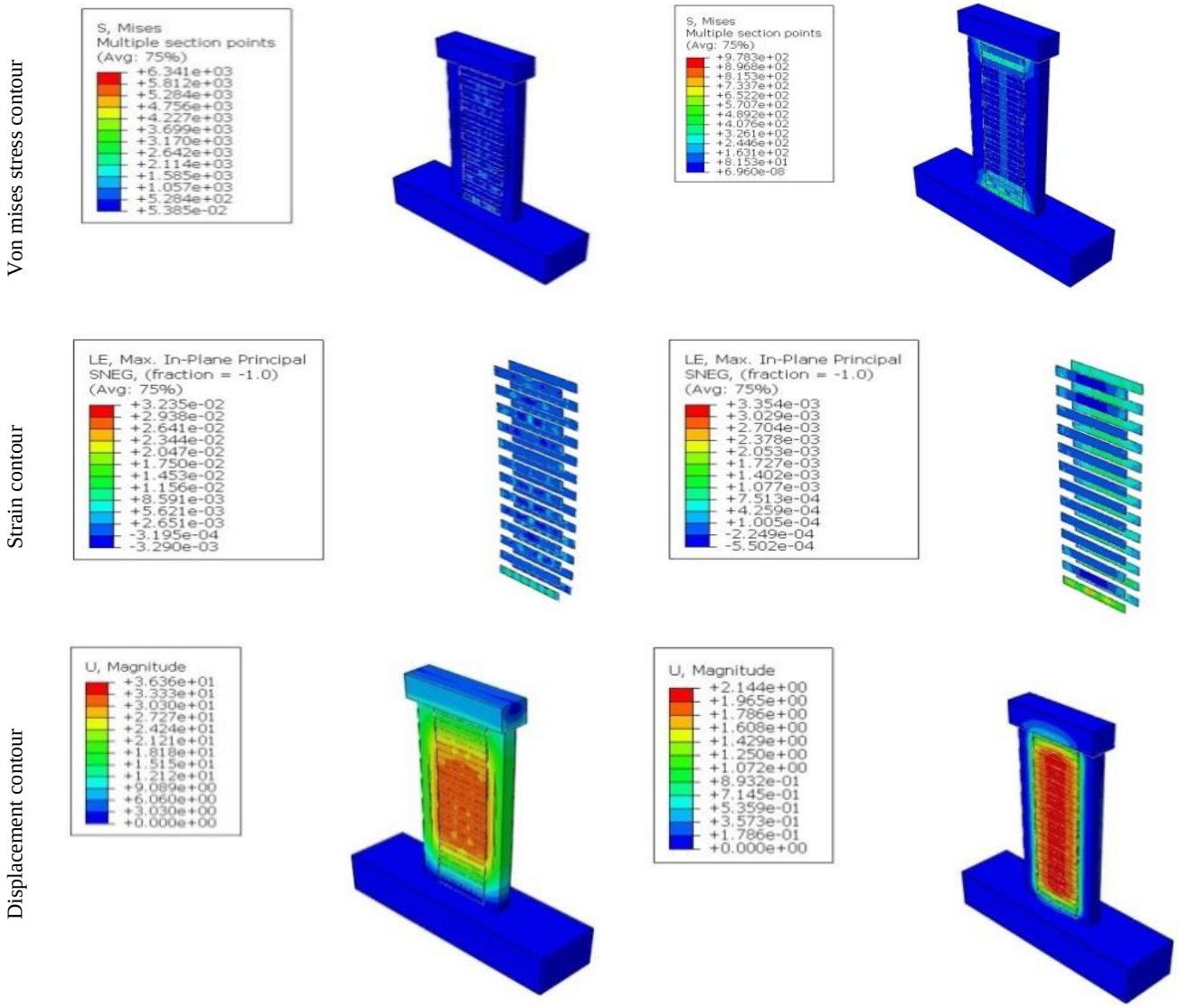

(a) Steel plate without holes (b) Steel plate with holes

Figure 20. Comparison of the effect of steel plate cross-sectional shape on a) stress, b) strain and c) displacement of composite shear wall with FRP sheets under blast load.

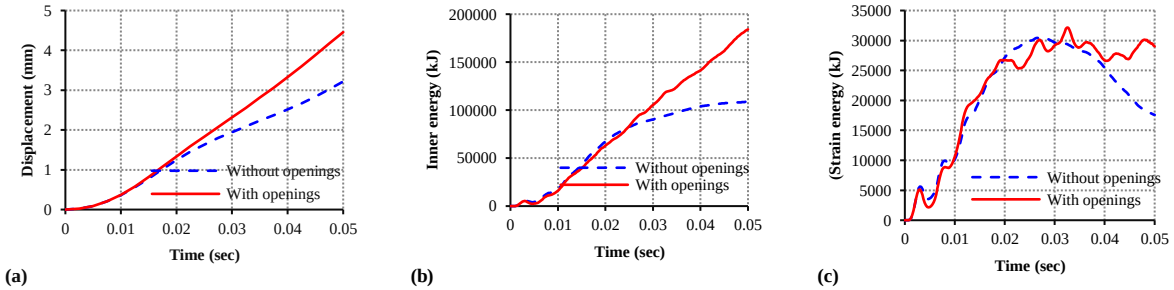

(a) (b) (c)

Figure 21. Comparison of the effect of steel plate cross-sectional shape on displacement and stored energy of FRP sheet-reinforced composite shear under blasting, a) displacement, b) inner energy, c) strain energy.

3.8. Impact of compressive strength of concrete

In this section, the effect of concrete compressive strength (f'c) on the performance of a composite shear wall reinforced with FRP strip under blast load is investigated. Figs. 22a to c show the results of the stress, strain and displacement contours created in the wall, for different values of f'c. The results show that with increasing f'c, the displacement decreases from 3.3 mm to 2.5 mm. The reason for this behavior is the presence of concrete surface, which leads to tensile and compressive yield of steel plate, almost simultaneously, and then if the concrete of the wall surface is not too thick, it is the tensile strips of steel plate that determine the behavior of the system.

The effect that the higher compressive strength of concrete has on the increase of strength and ductility of composite shear walls is due to later crushing of concrete. This indicates that increasing the compressive strength of concrete to a certain extent (f'c = 28 MPa) improves the performance of polymer fibers. The trend of displacement changes over time for different values of f'c is shown in Fig. 23a. Moreover, the results of changes in inner energy and strain energy generated in the composite shear wall for different values of f'C suggest that with increasing f'C, inner energy and strain energy also increase and in fact, using concrete with f'c = 28 (MPa) had the greatest effect on increasing the strength and ductility of the composite shear wall under the blast load.

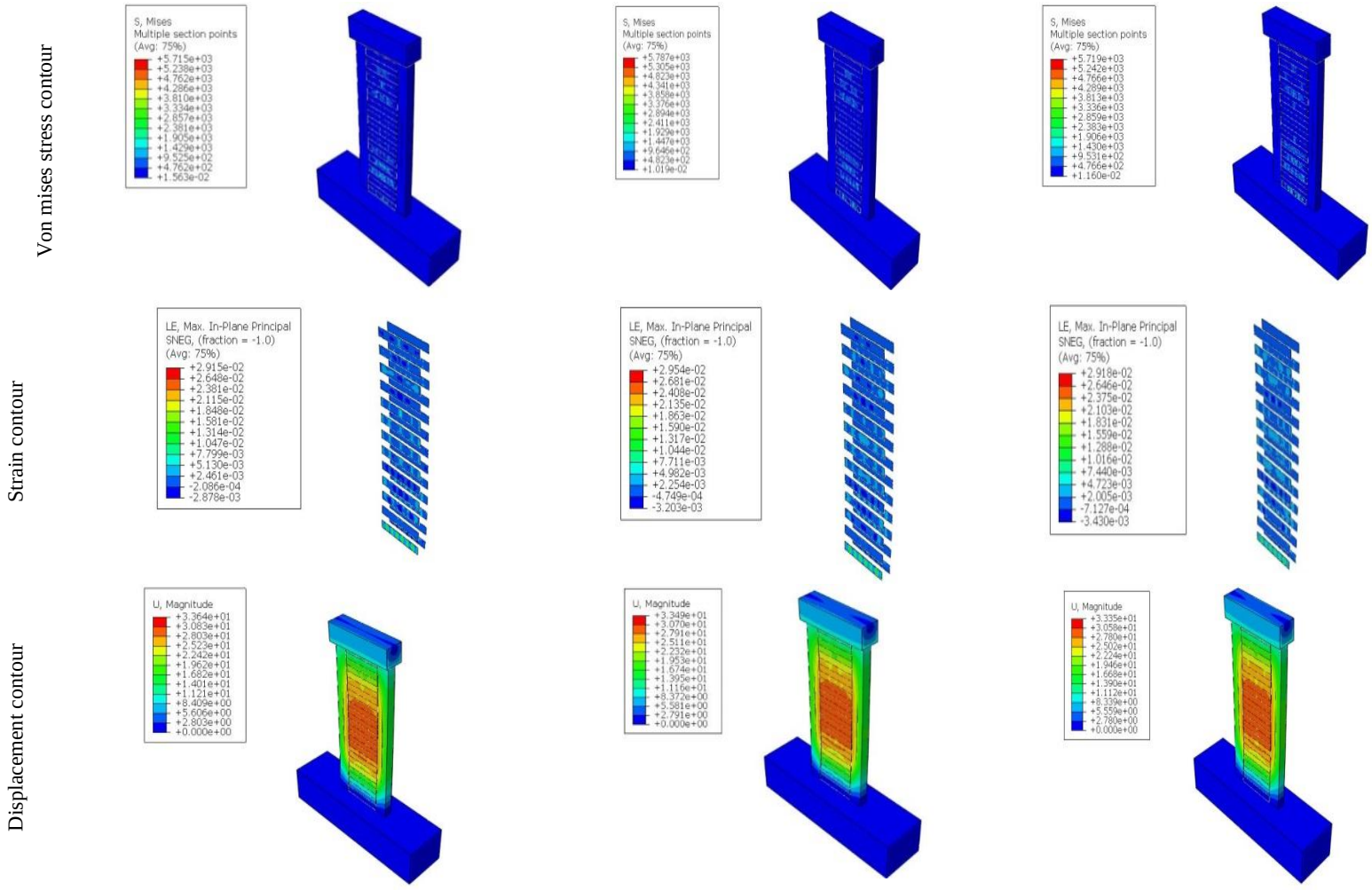

(a) f'_C = 21 MPa (b) f'_C = 28 MPa (c) f'_C = 35 MPa

Figure 22. Comparison of the effect of compressive strength of concrete on a) stress contours, b) strain and c) displacement of composite shear wall with FRP sheets under blast load.

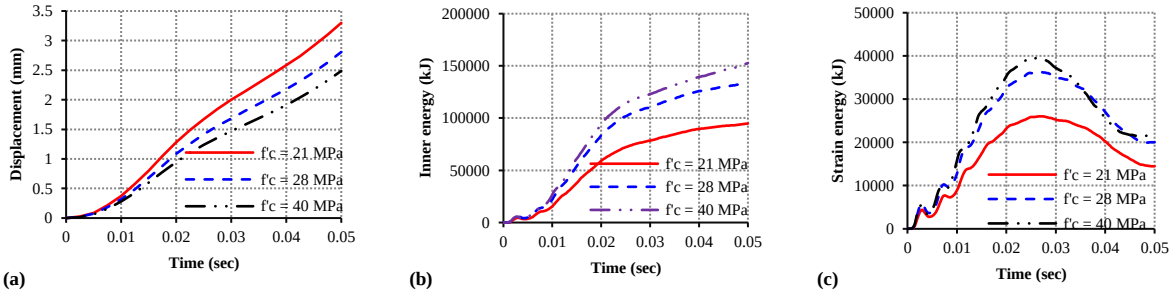

Figure 23. Comparison of the effect of concrete compressive strength on displacement and stored energy of composite shear wall with FRP sheets under blast effect, a) displacement, b) inner energy, c) strain energy.

4. Conclusions

In the present paper, the behavior of composite shear walls with FRP sheets under blast loads was investigated. The results of numerical modeling based on the FE method in ABAQUS can be summarized as follows:

1. Using FRP has increased the stress absorption in the wall, due to increased high load transfer capacity and high energy dissipation by polymer fibers. The analysis results also confirm that using FRP sheet can reduce wall displacement by 18.5%. This is because the use of FRP creates cohesion in the wall components and partially prevents the local collapse of the wall against blast, and to some extent also reduces the movement outside the wall plate. This effect delays the local rupture of the wall and is the main reason for the reduced displacement of the composite shear wall under the blast load.

2. CFRP and GFRP polymer sheets have the best and weakest performance in shear wall stress absorption, respectively. The high stiffness and modulus of elasticity of CFRP result in less displacement of the composite shear wall compared to the walls with other fibers. The amount of strain energy of the wall with CFRP sheets is higher by 28.59% than other fibers due to the high stiffness and hardness of carbon fibers compared to other fibers.

3. Similar trend was observed when the FRP sheet thickness was increased. By absorbing energy, the fibers prevent more concentration of stress in the composite shear wall and this effect increases with increasing fiber thickness. But as the thickness increases, the stiffness of the structure increases resulting in 41% increase in peak strain energy in 5mm thick laminate. Also, it was evident that increasing the thickness to a 5mm had positive influence. Increasing the thickness beyond 5mm showed negligible improvement.

4. The stresses, strains and displacements of the composite shear wall with FRP sheets with-holes steel plate are more than those with a without-holes sheet, due to the reduction of the strength of with-holes steel plate. The results also indicated that the perforation of the steel plate increased the inner energy by 71% but had no effect on the peak strain energy of the composite shear wall.

5. With the increase of the compressive strength of concrete, the stresses, strains and displacements of the composite shear wall with FRP sheets are first reduced and then increased. The reason for this behavior is the presence of concrete surface alone. Also, the effect of higher compressive strength of concrete on increasing the strength and ductility of composite shear walls can be described as the result of later crushing of concrete.

Author contributions: Investigation, Hosseini M and Li H; Conceptualization, Hosseini M and Li H; Funding acquisition, Hosseini M and Li H; Formal analysis, Hosseini M and Li H; Writing - original draft, Hosseini M and Li H; Supervision, Li H; review & editing, Hosseini A and Ghosh P.

Funding: The research work presented in this paper is supported by the Scientific Research Fund by Nanjing Forestry University (No. 163050206), Foreign Young Talents Project China (No. QN2021014006L), National Natural Science Foundation of China (Nos. 51878354 &51308301), Natural Science Foundation of Jiangsu Province (Nos. BK20181402 &

BK20130978),333 Talent High-Level Projects of Jiangsu Province and Qinglan Project of Jiangsu Higher Education Institutions. Any research results expressed in this paper are those of the writers and do not necessarily reflect the views of the foundations.

Acknowledgments: The writers gratefully acknowledge Ben Chen, Zhen Wang, Han Zhang, Ke Zhou,Xiaoyan Zheng, Shaoyun Zhu, Liqing Liu, Dunben Sun, Jing Cao, Yanjun Liu, Junhong Xu and othersfrom the Nanjing Forestry University for helping.

Conflicts of interest: The authors declare that they have no conflicts of interest to report regarding the present study.

References

Ajimituhuo, J. L., Abejide, O. S., & Mangut, S. (2018). Reliability analysis of CFRP shear walls subject to blast loading. Nigerian Journal of Technology, 37(3), 626–632.

Askarizadeh, N., & Mohammadizadeh, M. R. (2017). Numerical analysis of carbon fiber reinforced plastic (CFRP) shear walls and steel strips under cyclic loads using finite element method. Engineering, Technology & Applied Science Research, 7(6), 2147–2155.

Chen, L., Mahmoud, H., Tong, S.-M., & Zhou, Y. (2015). Seismic behavior of double steel plate–HSC composite walls. Engineering Structures, 102, 1–12.

Committee, A. C. I. (2008). Building code requirements for structural concrete (ACI 318-08) and commentary.

Dan, D. (2012). Experimental tests on seismically damaged composite steel concrete walls retrofitted with CFRP composites. Engineering Structures, 45, 338–348.

Epackachi, S., Nguyen, N. H., Kurt, E. G., Whittaker, A. S., & Varma, A. H. (2014). Numerical and experimental investigation of the in-plane behavior of rectangular steel-plate composite walls. Structures Congress 2014, 2478–2487.

Goel, M. D., & Matsagar, V. A. (2014). Blast-resistant design of structures. Practice Periodical on Structural Design and Construction, 19(2), 04014007.

Jayasooriya, J., Thambiratnam, D., Perera, N., & Kosse, V. (2009). Response and damage evaluation of reinforced concrete frames subjected to blast loading. Proceedings of the 34th Conference on Our World in Concrete & Structures-Conference Documentation Volume XXVIII, 123–130.

Hosseini, M., Jian, B., Li, H., Yang, D., Wang, Z. et al. (2022). A Review of Fibre Reinforced Polymer (FRP) Reinforced Concrete Composite Column Members Modelling and Analysis Techniques. Journal of Renewable Materials, 10(12), 3243–3262.

Wilt, J., GangaRao, H., Liang, R. F., & Mostoller, J. (2023). Structural responses of FRP sheet piles under cantilever loading. Sustainable Structures, 3(1), 000021.

Mohamed, T., Elshazli, N. S., & Ahmed, I. (2022). Structural response of high strength concrete beams using fiber reinforced polymers under reversed cyclic loading. Sustainable Structures, 2(2), 000018.

Liang, R., & Hota, G. (2021). Development and evaluation of load-bearing fiber reinforced polymer composite panel systems with tongue and groove joints. Sustainable Structures, 1(2), 000008

Mutalib, A.A., & Hao, H. (2011). Numerical analysis of FRP-composite-strengthened RC panels with anchorages against blast loads. Journal of Performance of Constructed Facilities, 25(5), 360-372.

Ji, X., Jiang, F., & Qian, J. (2013). Seismic behavior of steel tube–double steel plate–concrete composite walls: Experimental tests. Journal of Constructional Steel Research, 86, 17–30.

Khizab, B., Sadeghi, A., Hashemi, S. V., Mehdizadeh, K., & Nasseri, H. (2021). Investigation the performance of Dual Systems Moment-Resisting Frame with Steel Plate Shear Wall Subjected to Blast Loading. Journal of Structural and Construction Engineering, 8(8), 102–127.

Kulak, G. L., Grondin, G. Y., Adams, P. F., & Krentz, H. A. (1998). Limit states design in structural steel. Canadian Institute of Steel Construction.

Liang, Q. Q. (2009). Strength and ductility of high strength concrete-filled steel tubular beam–columns. Journal of Constructional Steel Research, 65(3), 687–698.

Mander, J. B., Priestley, M. J., & Park, R. (1988). Theoretical stress-strain model for confined concrete. Journal of Structural Engineering, 114(8), 1804–1826.

Moghimi, H., & Driver, R. G. (2015). Performance assessment of steel plate shear walls under accidental blast loads. Journal of Constructional Steel Research, 106, 44–56.

Nie, J.-G., Hu, H.-S., Fan, J.-S., Tao, M.-X., Li, S.-Y., & Liu, F.-J. (2013). Experimental study on seismic behavior of high-strength concrete filled double-steel-plate composite walls. Journal of Constructional Steel Research, 88, 206–219.

Hosseini, M., Bingyu, J., Jian, Z., Li, H., Lorenzo, R., et al. (2023). Numerical Study on the behaviour of Hybrid FRPs Reinforced RC Slabs Subjected to Blast Loads. Journal of Renewable Materials, 11(9), 1-15.

Nie, J.-G., Ma, X.-W., Tao, M.-X., Fan, J.-S., & Bu, F.-M. (2014). Effective stiffness of composite shear wall with double plates and filled concrete. Journal of Constructional Steel Research, 99, 140–148.

Nguyen, N. H. (2016). Seismic response of steel-plate concrete composite shear wall piers. State University of New York at Buffalo.

Shabanlou, M., Moghaddam, H., & Saedi Daryan, A. (2021). The Effect of Geometry on Structural Behavior of Buildings with Steel Plate Shear Wall System Subjected to Blast Loading. International Journal of Steel Structures, 21(2), 650–665.

Shirinzadeh, M., & Haghollahi, A. (2016). Performance of shear wall with external reinforcement by CFRP and steel sheets against blast load. Journal of Vibroengineering, 18(5), 2735–2743.

Thorburn, L. J., Montgomery, C. J., & Kulak, G. L. (1983). Analysis of steel plate shear walls.

Timothy, P., McCormick , P.E. (2010) "Shear Walls guideline, Seismic Retrofit Training",New-Jersey,

Wagner, H. (1935). Tension fields in originally curved, thin sheets during shearing stresses (Issue 774). National Advisory Commitee for Aeronautics.

Warn, G. P., & Bruneau, M. (2009). Blast resistance of steel plate shear walls designed for seismic loading. Journal of Structural Engineering, 135(10), 1222–1230.

Zhao, Q., & Astaneh-Asl, A. (2004). Cyclic behavior of traditional and innovative composite shear walls. Journal of Structural Engineering, 130(2), 271–284.

Zhao, W., Guo, Q., Huang, Z., Tan, L., Chen, J., & Ye, Y. (2016). Hysteretic model for steel–concrete composite shear walls subjected to in-plane cyclic loading. Engineering Structures, 106, 461–470.

Zhang, X., Qin, Y., & Chen, Z. (2016). Experimental seismic behavior of innovative composite shear walls. Journal of Constructional Steel Research, 116, 218–232.